JACS
JOURNAL OF THE AMERICAN CHEMICAL SOCIETY

Communication

pubs.acs.org/JACS

Bottom-up Construction of a Primordial Carboxysome Mimic

Raphael Frey,[‡] Shiksha Mantri,[‡] Marco Rocca, and Donald Hilvert*

Laboratory of Organic Chemistry, ETH Zurich, 8093 Zurich, Switzerland

Supporting Information

ABSTRACT: We have constructed a synthetic mimic of the carboxysome, a cyanobacterial carbon-fixing organelle. Using an electrostatic tagging system, we coencapsulated the two key carboxysomal enzymes, ribulose-1,5-bisphosphate carboxylase/oxygenase (RuBisCO) and carbonic anhydrase (CA), in an engineered protein cage based on lumazine synthase. A statistically significant kinetic effect of coencapsulated CA on RuBisCO activity was not observed under ambient or oxygen saturated conditions, suggesting that enzyme proximity alone may not be the key determinant in carboxysome function. The capsid shell protected the enzyme from proteolytic damage, a factor that could have provided early cyanobacteria with an evolutionary benefit. Our strategy to coencapsulate different proteins can easily be extended to other sequentially acting enzymes and lays down principles for developing artificial organelles to control biosynthetic pathways *in vivo*.

Cells carry out simultaneous orthogonal reactions by encapsulating sets of enzymes involved in a metabolic pathway in lipid or protein-bound subcellular structures.[1] Compartmentalization of sequentially acting enzymes is proposed to lead to significant rate enhancements due to high local concentrations of enzymes, substrates, and cofactors, and intermediate channeling.[2] Additionally, there is evidence that in some bacterial microcompartments (BMCs), such as the propanediol and ethanolamine utilizing microcompartments, the encasing protein shell acts as a diffusional barrier, limiting the escape of toxic aldehyde intermediates to the cytosol.[3] BMCs and other protein cages have received recent attention with the prospect of utilizing them for enzyme encapsulation to construct designer organelles.[4−6]

The most studied BMC is the carboxysome, the carbon fixing organelle of cyanobacteria, which performs the final step in the carbon concentrating mechanism (CCM).[7] The carboxysome is composed of a complex protein shell that encapsulates the enzymes CA and RuBisCO. CA converts hydrogen carbonate (HCO_3^-), which enters the carboxysome from the cytoplasm, to CO_2 in the vicinity of RuBisCO. RuBisCO fixes the locally produced CO_2 to a molecule of ribulose-1,5-bisphosphate (RuBP) to produce two molecules of 3-phosphoglycerate (3-PGA). Besides providing high internal concentrations of CO_2, the shell ostensibly acts as a barrier to O_2, which is a competitive substrate for RuBisCO.[8]

It is hypothesized that carboxysomes arose ∼3.5 billion years ago in response to steadily dropping atmospheric CO_2/O_2 ratios.[9] Two types of carboxysomes, α and β, evolved convergently. While CA is associated with the inner surface of the shell in both compartments, they differ considerably in their RuBisCO packing. β-Carboxysomes, which purportedly originated from a closely packed core of RuBisCO and CA, have a densely packed lumen with RuBisCO enzymes arranged in a three-dimensional array by a scaffolding protein. In contrast, α-carboxysomes have less internal organization, with layers of RuBisCO packed against the inside of the shell and some RuBisCO loosely located in the interior. α-Carboxysomes are believed to have arisen from RuBisCO and CA enzymes that invaded existing BMC structures by exploiting targeting peptides.[9] The different internal organization but similar carbon fixing properties of α- and β-carboxysomes[10] suggests that there are no stringent structural requirements for a functional carbon-fixing organelle.

In line with the proposed structure of early α-carboxysomes, we envisaged constructing a simple carboxysome mimic in a bottom-up fashion using a protein cage to coencapsulate RuBisCO and CA enzymes (Figure 1). Such a model could

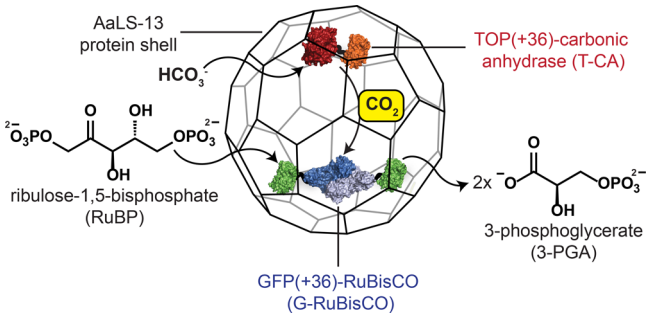

Figure 1. Schematic representation of an artificial carboxysome (not drawn to scale).

potentially provide insight into the early evolutionary benefits achieved by colocalization of RuBisCO and CA and thus lead to a better understanding of carboxysome function in general. As the protein shell for the construction of our carboxysome mimic we chose an engineered variant of a lumazine synthase from *Aquifex aeolicus*, AaLS-13, which contains a negatively charged lumenal surface and encapsulates positively charged cargo *in vitro* and *in vivo*.[11−13]

Positively supercharged variants of green and yellow fluorescent proteins, GFP(+36) and TOP(+36), have been shown to be efficient tags for directing monomeric and dimeric enzymes to the interior of AaLS-13 capsids.[14,15] In order to use

Received: May 8, 2016
Published: August 1, 2016

DOI: 10.1021/jacs.6b04744
J. Am. Chem. Soc. 2016, 138, 10072−10075

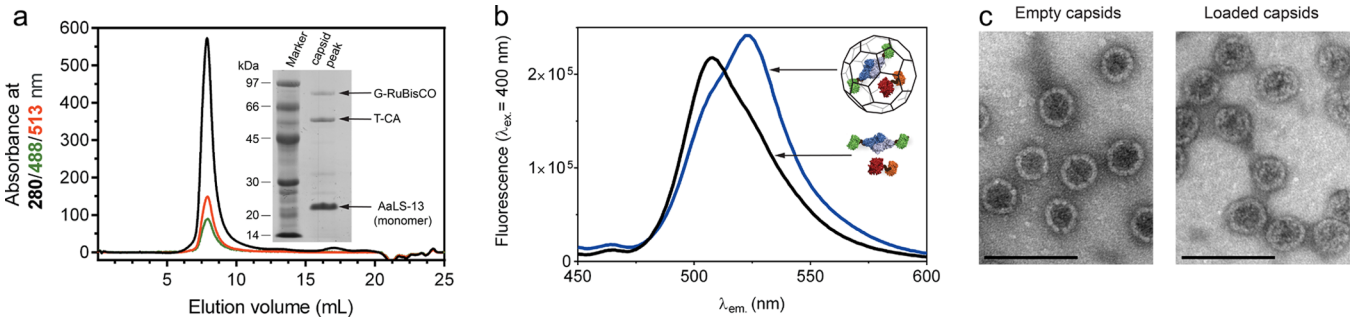

Figure 2. Assembling a carboxysome mimic. (a) Size exclusion chromatogram of AaLS-13 capsids mixed with G-RuBisCO and T-CA. Inset: SDS-PAGE of capsid peak confirming the coelution of G-RuBisCO and T-CA with AaLS-13. (b) Fluorescence traces of free (black) and encapsulated (blue) G-RuBisCO and T-CA in a 1:5 ratio excited at λ = 400 nm. (c) Negative stain TEM of empty and filled capsids; assuming a 180-mer T = 3 structure,[11] the loaded AaLS-13 cages contain 38 guests (scale bar: 100 nm).

this strategy for the encapsulation of RuBisCO and CA, a dimeric, noncarboxysomal RuBisCO from the proteobacterium *Rhodospirillum rubrum* and a monomeric CA from *Homo sapiens* (hCAII) were chosen. The activities of these enzymes are similar to those reported for carboxysomal RuBisCO and CA variants (Table S1). RuBisCO and hCAII were genetically fused to GFP(+36) and TOP(+36) to yield the constructs G-RuBisCO and T-CA, respectively (Figure 1). RuBisCO activity was measured using radiometric and spectrophotometric assays, and the esterase activity of CA was determined spectrophotometrically using *p*-nitrophenyl acetate as the substrate. The fusion constructs retained high activities, showing only ∼2-fold lower k_{cat}/K_M values than the wild-type enzymes (Tables S2 and S3).

G-RuBisCO and T-CA were encapsulated by mixing the enzymes with AaLS-13 capsids in different stoichiometric ratios (Figure S1). The host−guest complexes were purified by size exclusion chromatography (SEC). Coelution of the enzymes with the capsid was confirmed by SDS-PAGE (Figure 2a). Absorption of the fluorophores at 488 and 513 nm was used to determine the concentrations of G-RuBisCO and T-CA, respectively (Figure S2). No significant differences in the sizes of empty and filled capsids were found when the particles were examined by negative stain transmission electron microscopy (TEM). The average outer diameter of capsids containing 38 guests was 37 ± 2 nm (n = 20), identical to empty capsids (Figures 2c and S3).

Förster resonance energy transfer (FRET) between the fluorescent GFP(+36) and TOP(+36) tags confirmed coencapsulation of the guest enzymes (Figure 2b). While a mixture of free G-RuBisCO and T-CA in solution did not show any FRET, encapsulated samples with the same concentration of G-RuBisCO and T-CA displayed FRET signals that depended on the ratio between the fluorescent GFP(+36) donor and TOP(+36) acceptor as well as the total number of guests per capsid.[15] This result confirms the close proximity of G-RuBisCO and T-CA upon coencapsulation inside AaLS-13 and allowed us to investigate how such an arrangement affects catalytic activity.

Activity was first tested for each enzyme encapsulated separately. In contrast to examples of other enzymes sequestered in protein cages,[14,16,17] we found that the activity of G-RuBisCO was slightly enhanced upon localization in the lumen of AaLS-13, whereas the activity of T-CA remained essentially unchanged (Tables 1, S2, and S3). In the case of RuBisCO, encapsulation may stabilize the enzyme's dimeric structure as was recently shown for a heterodimeric hydrogenase encapsulated in bacteriophage P22 capsids.[18]

Table 1. Kinetic Parameters of Free, Encapsulated and Co-Encapsulated G-RuBisCO[a]

	k_{cat} (s^{-1})	$K_{M,\ HCO_3^-}$ (mM)	k_{cat}/K_M ($M^{-1}\ s^{-1}$)
free G-RuBisCO	1.6 ± 0.3	35 ± 12	46 ± 18
AaLS-13 + G-RuBisCO	1.9 ± 0.2	23 ± 5	83 ± 20
AaLS-13 + G-RuBisCO + T-CA	2.5 ± 0.3	27 ± 6	93 ± 23
AaLS-13 + G-RuBisCO + T-CA + CA-inhibitor	2.3 ± 0.3	23 ± 7	100 ± 33

[a]Values are the mean ± standard deviation ($n \geq 3$). Activity was determined under ambient air conditions at pH 8.0 and [RuBP] = 250 μM using a radiometric assay.[23] Capsid−guest complexes were purified by SEC before assaying for RuBisCO activity. For additional experimental details and kinetic data, see SI Materials and Methods and Table S2.

When G-RuBisCO was coencapsulated with T-CA, the k_{cat} for the carboxylation reaction increased somewhat (∼1.3-fold), but the apparent K_M for HCO_3^- did not change (Table 1, Figure 3a). In an analogous study with natural carboxysomes, the k_{cat} of RuBisCO contained in complete carboxysomes was 1.3−1.7 times higher compared to RuBisCO in carboxysome mutants lacking CA enzymes, and the apparent K_M for CO_2 was 3 times lower.[19] To explore the effect of coencapsulated CA more directly, we used a high affinity CA inhibitor, acetazolamide,[20] to inhibit the activity of T-CA in capsid samples containing both enzymes. No apparent difference in RuBisCO activity was observed upon decreasing CA activity more than 4 orders of magnitude, implying that the carbonic anhydrase activity of coencapsulated T-CA is not responsible for the marginal rate enhancement observed for RuBisCO. Similarly, no differences were observed when the carboxysome mimics were assayed in a more alkaline environment (pH = 9.2). Despite lowering the CO_2 to HCO_3^- ratio, carbon fixation was not enhanced by the presence of CA under these conditions.[21]

In natural carboxysomes, the RuBisCO/CA ratio is tightly controlled and may be important for efficient channeling of intermediates.[9] We therefore assayed encapsulated RuBisCO at G-RuBisCO/T-CA ratios ranging from 1:20 to 3:1. In our system, RuBisCO activity was found to be independent of both the ratio and the total number of encapsulated enzymes (Figures S4 and S5).

DOI: 10.1021/jacs.6b04744
J. Am. Chem. Soc. 2016, 138, 10072−10075

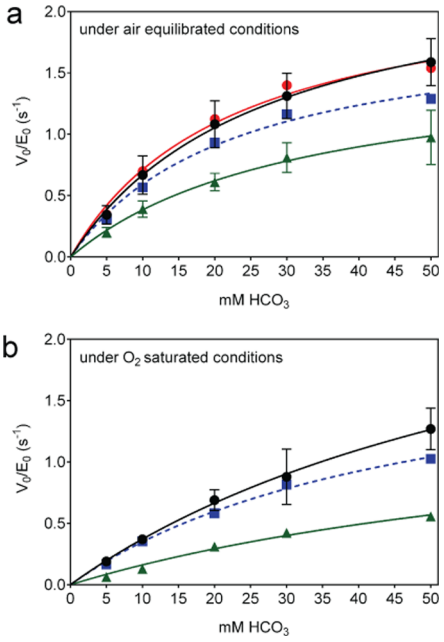

Figure 3. Michaelis–Menten plots of free G-RuBisCO (green), encapsulated G-RuBisCO (dashed blue), and coencapsulated G-RuBisCO and T-CA (black: without CA inhibitor, red: with CA inhibitor) in (a) air and (b) O_2 saturated environments ($n \geq 3$).

With free RuBisCO, RuBP can react with either CO_2 or O_2, whereas RuBisCO sequestered in carboxysomes is less susceptible to the undesired oxygenase reaction.[22] To test the reactivity of the artificial carboxysome with O_2, we compared the activity of free and encapsulated G-RuBisCO with and without coencapsulated T-CA in air-equilibrated and O_2 saturated buffers. The k_{cat}/K_M for RuBP carboxylation catalyzed by the free enzyme decreased 2.9-fold in buffer saturated with O_2 versus air. For comparison, the k_{cat}/K_M of encapsulated G-RuBisCO and the coencapsulated enzymes decreased by 2.3- and 1.9-fold, respectively, under the same conditions (Figure 3b, Table S4). Although the AaLS-13 shell may provide a small protective effect, it clearly does not prevent encapsulated RuBisCO from reacting with O_2 and cannot be considered an efficient diffusion barrier to gaseous molecules such as CO_2 and O_2.

In the absence of a significant kinetic advantage, embedding metabolically important enzymes within a simple protein shell could have provided other benefits such as resistance to thermal or proteolytic degradation.[17] Carboxysomes evolved when cells were subject to intense irradiation and severe oxidative stress, conditions that promote oxidation and proteolysis of cytoplasmic proteins.[24] To test whether the presence of the AaLS-13 protein shell protects the encapsulated enzymes from proteolysis, we treated the free and encapsulated enzymes with the protease Factor Xa, which has high specificity for the sequence just before the linker of the GFP(+36)-enzyme fusions. After 1 h, the free enzyme was completely truncated, whereas the encapsulated enzyme was only partially cleaved (Figures 4 and S6). Proteolysis in the latter case may occur upon passive encapsulation of the protease or dissociation of G-RuBisCO from the capsid.[15]

Our artificial carboxysome, which was designed to mimic primordial α-carboxysomes, allowed us to investigate potential evolutionary benefits of colocalizing RuBisCO and CA, presumably a key event in the evolution of carboxysomes.

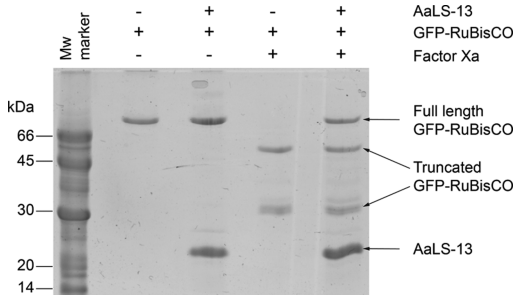

Figure 4. SDS-PAGE showing free G-RuBisCO and encapsulated enzyme in a sample containing 33 guests/capsid before and after treatment with Factor Xa at a final concentration of 42 μg/mL for 1 h at room temperature. The concentration of G-RuBisCO was 3 μM in each sample.

Even though quite high packing densities of up to 5 mM were achieved inside AaLS-13, the resulting proximity to CA did not enhance RuBisCO activity. A recent study suggested that efficient channeling of intermediates between two enzymes requires very dense and rather large clusters.[25] Modern α-carboxysomes have effective RuBisCO concentrations of about 12 mM and are roughly 3 times larger than AaLS-13. The surrounding protein shell of α-carboxysomes is also much more complex than that of AaLS-13, consisting of many components that may be important for regulating substrate flux and controlling relative permeability to CO_2 and O_2.[26] Another difference is the internal organization of the enzymes in the protein cages. In AaLS-13, guests are exclusively associated with the interior wall of the capsid due to electrostatic interactions, whereas, in α-carboxysomes, CA is associated with the capsid wall and RuBisCO is packed both against the inside of the shell and in the lumen.[9] In addition to enzyme colocalization and organization, intermediate channeling may also depend on well matched enzyme efficiencies.[27]

Calculations by Badger et al. indicate that the effects of coencapsulated CA should become evident only at high HCO_3^-/CO_2 ratios.[21] In cyanobacteria, HCO_3^- ions are actively pumped into the cytosol by energy driven pumps leading to a HCO_3^-/CO_2 ratios that are ~20-times higher than under typical assay conditions *in vitro*.[21,28] This finding suggests that an artificial carboxysome may evince little advantage *in vitro* but might nevertheless increase the rate of CO_2 fixation *in vivo*. Production of synthetic carboxysomes together with HCO_3^- ion pumps in hosts such as *E. coli* could thus conceivably enable heterotrophic carbon fixation and sustainable production of high-value chemicals.[29−31] The simple design of our artificial carboxysomes may circumvent issues associated with expression of natural carboxysomes in heterologous hosts, where fine-tuning of multiple components is crucial but difficult to control.[29] Moreover, since all components of our primordial carboxysome are evolvable, further optimization through directed evolution is also conceivable.[11,32,33]

The construction of an artificial carboxysome using the AaLS-13 encapsulation system illustrates a facile means of coencapsulating two or more kinds of enzymes, a general strategy that could be extended to diverse enzyme couples, laying the path for creating other artificial organelles. Considering the moderate kinetic effects that we observed for a reaction sequence involving low molecular weight species, encapsulation of an enzyme cascade acting on macromolecular

DOI: 10.1021/jacs.6b04744
J. Am. Chem. Soc. 2016, 138, 10072−10075

substrates and intermediates that are more likely to be contained inside the protein shell might show higher rate enhancements.

■ ASSOCIATED CONTENT

Supporting Information

The Supporting Information is available free of charge on the ACS Publications website at DOI: 10.1021/jacs.6b04744.

Complete experimental procedures, tables with catalytic parameters, and additional figures (PDF)

■ AUTHOR INFORMATION

Corresponding Author

*hilvert@org.chem.ethz.ch

Author Contributions

‡R.F. and S.M. contributed equally and are listed alphabetically.

Notes

The authors declare no competing financial interest.

■ ACKNOWLEDGMENTS

We thank Peter Tittmann at the Scientific Center for Optical and Electron Microscopy (ScopeM, ETH Zurich), Dr. Eita Sasaki for assistance with electron microscopy experiments, and Dr. Martin Badertscher for help with the radiometric assay. This work was generously supported by the ETH Zurich and the European Research Council (Advanced ERC Grant ERC-dG-2012-321295 to D.H.).

■ REFERENCES

(1) Kerfeld, C. A.; Heinhorst, S.; Cannon, G. C. *Annu. Rev. Microbiol.* **2010**, *64*, 391−408.
(2) Siu, K.; Chen, R. P.; Sun, Q.; Chen, L.; Tsai, S.; Chen, W. *Curr. Opin. Biotechnol.* **2015**, *36*, 98−106.
(3) Yeates, T. O.; Crowley, C. S.; Tanaka, S. *Annu. Rev. Biophys.* **2010**, *39*, 185−205.
(4) Chen, A. H.; Silver, P. A. *Trends Cell Biol.* **2012**, *22*, 662−670.
(5) Kim, E. Y.; Tullman-Ercek, D. *Curr. Opin. Biotechnol.* **2013**, *24*, 627−632.
(6) Bobik, T. A.; Lehman, B. P.; Yeates, T. O. *Mol. Microbiol.* **2015**, *98*, 193−207.
(7) Yeates, T. O.; Kerfeld, C. A.; Heinhorst, S.; Cannon, G. C.; Shively, J. M. *Nat. Rev. Microbiol.* **2008**, *6*, 681−691.
(8) Cannon, G. C.; Bradburne, C. E.; Aldrich, H. C.; Baker, S. H.; Heinhorst, S.; Shively, J. M. *Appl. Environ. Microbiol.* **2001**, *67*, 5351−5361.
(9) Rae, B. D.; Long, B. M.; Badger, M. R.; Price, G. D. *Microbiol. Mol. Biol. Rev.* **2013**, *77*, 357−379.
(10) Whitehead, L.; Long, B. M.; Price, G. D.; Badger, M. R. *Plant Physiol.* **2014**, *165*, 398−411.
(11) Wörsdörfer, B.; Woycechowsky, K. J.; Hilvert, D. *Science* **2011**, *331*, 589−592.
(12) Wörsdörfer, B.; Pianowski, Z.; Hilvert, D. *J. Am. Chem. Soc.* **2012**, *134*, 909−911.
(13) Seebeck, F. P.; Woycechowsky, K. J.; Zhuang, W.; Rabe, J. P.; Hilvert, D. *J. Am. Chem. Soc.* **2006**, *128*, 4516−4517.
(14) Azuma, Y.; Zschoche, R.; Tinzl, M.; Hilvert, D. *Angew. Chem., Int. Ed.* **2016**, *55*, 1531−1534.
(15) Zschoche, R.; Hilvert, D. *J. Am. Chem. Soc.* **2015**, *137*, 16121−16132.
(16) Patterson, D. P.; Prevelige, P. E.; Douglas, T. *ACS Nano* **2012**, *6*, 5000−5009.
(17) Fiedler, J. D.; Brown, S. D.; Lau, J. L.; Finn, M. G. *Angew. Chem., Int. Ed.* **2010**, *49*, 9648−9651.
(18) Jordan, P. C.; Patterson, D. P.; Saboda, K. N.; Edwards, E. J.; Miettinen, H. M.; Basu, G.; Thielges, M. C.; Douglas, T. *Nat. Chem.* **2016**, *8*, 179−185.
(19) Dou, Z.; Heinhorst, S.; Williams, E. B.; Murin, C. D.; Shively, J. M.; Cannon, G. C. *J. Biol. Chem.* **2008**, *283*, 10377−10384.
(20) Innocenti, A.; Scozzafava, A.; Parkkila, S.; Puccetti, L.; De Simone, G.; Supuran, C. T. *Bioorg. Med. Chem. Lett.* **2008**, *18*, 2267−2271.
(21) Badger, M. R.; Price, G. D.; Yu, J. W. *Can. J. Bot.* **1991**, *69*, 974−983.
(22) Marcus, Y.; Berry, J. A.; Pierce, J. *Planta* **1992**, *187*, 511−516.
(23) Badger, M. R.; Price, G. D. *Plant Physiol.* **1989**, *89*, 51−60.
(24) Cabiscol, E.; Tamarit, J.; Ros, J. *Internatl. Microbiol.* **2000**, *3*, 3−8.
(25) Castellana, M.; Wilson, M. Z.; Xu, Y.; Joshi, P.; Cristea, I. M.; Rabinowitz, J. D.; Gitai, Z.; Wingreen, N. S. *Nat. Biotechnol.* **2014**, *32*, 1011−1018.
(26) Kinney, J. N.; Axen, S. D.; Kerfeld, C. A. *Photosynth. Res.* **2011**, *109*, 21−32.
(27) Patterson, D. P.; Schwarz, B.; Waters, R. S.; Gedeon, T.; Douglas, T. *ACS Chem. Biol.* **2014**, *9*, 359−365.
(28) Price, G. D.; Badger, M. R.; Woodger, F. J.; Long, B. M. *J. Exp. Bot.* **2007**, *59*, 1441−1461.
(29) Bonacci, W.; Teng, P. K.; Afonso, B.; Niederholtmeyer, H.; Grob, P.; Silver, P. A. *Proc. Natl. Acad. Sci. U. S. A.* **2012**, *109*, 478−483.
(30) Gong, F.; Liu, G.; Zhai, X.; Zhou, J.; Cai, Z.; Li, Y. *Biotechnol. Biofuels* **2015**, *8*, 86.
(31) Guadalupe-Medina, V.; Wisselink, H. W.; Luttik, M. A.; de Hulster, E.; Daran, J.-M.; Pronk, J. T.; van Maris, A. J. *Biotechnol. Biofuels* **2013**, *6*, 125.
(32) Mueller-Cajar, O.; Morell, M.; Whitney, S. M. *Biochemistry* **2007**, *46*, 14067−14074.
(33) Boone, C. D.; Habibzadegan, A.; Gill, S.; McKenna, R. *Biomolecules* **2013**, *3*, 553−562.

DOI: 10.1021/jacs.6b04744
J. Am. Chem. Soc. 2016, 138, 10072−10075